ELSEVIER

Journal of Power Sources 107 (2002) 67–73

JOURNAL OF POWER SOURCES

www.elsevier.com/locate/jpowsour

Effect of carbon monoxide on the electrooxidation of hydrogen by tungsten carbide

D.R. McIntyre, G.T. Burstein*, A. Vossen

Department of Materials Science, University of Cambridge, Pembroke Street, Cambridge CB2 3QZ, UK

Received 3 August 2001; received in revised form 15 October 2001; accepted 20 October 2001

Abstract

The effect of carbon monoxide (CO) on the anodic oxidation of hydrogen by tungsten carbide (WC) electrocatalysts is described. CO poisoning of these base electrocatalysts is small, with reductions of $\leq$6% of the hydrogen current. Tests of the anodic oxidation of CO alone on these catalysts show the reaction to be very slow. The low degree of poisoning is quite reversible and ascribed to weak adsorption of CO on WC surfaces. The experiments have been conducted on a variety of WCs synthesised from several different routes, all showing similar results.

Keywords: Base electrocatalysts; Carbon monoxide; Fuel cells; Hydrogen oxidation; Poisoning; Tungsten carbide

1. Introduction

The presently unfavourable economics of fuel cells would be greatly improved if these devices could use cheap fuels and low-cost catalysts. One common and relatively cheap fuel is reformate hydrogen made by steam reformation of hydrocarbons into mixtures of hydrogen and the oxides of carbon.

The CO_2 in reformate hydrogen would quickly lead to carbonate build-up and loss of conductivity in any alkaline electrolyte [1], so reformate hydrogen is ill-suited for use in alkaline fuel cells. Acidic electrolytes reject CO_2 [2]. However, carbon monoxide (CO) is a severe poison on the platinum catalysts most commonly used in fuel cells; at 160 °C the 2% CO typically found in reformate H_2 fuel reduces the current drawn from a Pt anode by two orders of magnitude [3]. With Pt electrocatalysts, even 100 ppm of CO in a H_2 gas stream reduces the current output of a fuel cell by about 80% in practical potential ranges [4] as the CO adsorbs strongly onto active Pt sites, blocking further reaction. Because of the CO poisoning effect, Pt–Ru alloy anode catalysts have been proposed [5]. Hydrogen processing devices to reduce the CO content in the H_2 to well below 100 ppm have been developed [6] but these impose significant penalties in energy efficiency, system start-up time and complexity [7].

Researchers have made strong, if sporadic, efforts to identify cheaper substitutes for the platinum-based catalysts on which virtually all fuel cells now rely. For use as anode electrocatalysts in acidic environments, tungsten carbide (WC) and modifications thereof, have been cited as possibilities [8–14] (WC has been identified as a H_2 evolution catalyst as well [15]). One reason for the abiding interest in WC is that early workers in the field reported it to be ''completely resistant'' [9] or ''immune'' [10,11] to CO poisoning at all concentrations. However, experimental data in support of these statements are limited. The electrocatalytic activity of WC is highly sensitive to the synthesis technique [16], but no studies have reported how the CO resistance of WC might vary as a function of synthesis method. In this paper, we examine the effect of CO on the anodic oxidation of H_2 on WC derived from several synthesis routes and demonstrate that CO poisoning, although detectable, is small and reversible.

2. Experimental procedure

2.1. Synthesis

A commercial WC powder (labelled sample I) was obtained (Johnson–Matthey (JM) reagent grade, 99.5% WC) and tested as received. Four other WC samples (labelled II–V) were synthesised by thermal treatment of precursor compounds in mixed gases [17]. Precursors for the thermal treatments were:

* Corresponding author. Tel.: +44-1223-334-361; fax: +44-1223-334-567.
E-mail address: gtb1000@cus.cam.ac.uk (G.T. Burstein).

0378-7753/02/$ – see front matter
PII: S0378-7753(01)00987-9

- sample II: WO_3 (Aldrich, 99+%),
- sample III: co-precipitated Co–W alloy of 1:2 mole ratio (1Co2W),
- sample IV: peroxopolytungstic acid (PPTA)
- sample V: $NiWO_4$ (Alfa, 99+%).

2.1.1. 1Co2W alloy precursor

The co-precipitated 1Co2W precursor was made as follows: 0.0525 mol (9.6534 g) of metallic W powder (Alfa, 99.9%) was dissolved [18] at room temperature in 50% H_2O/50% H_2O_2 (v/v) (note: the W powder must be added slowly, in 1 or 2 g increments, to the H_2O_2 solution with continuous magnetic stirring. The dissolution is exothermic. Adding the powder too quickly can result in the solution boiling over). To this solution was added 0.0262 mol of Co as a solution of 7.6688 g $Co(NO_3)_2{\cdot}6H_2O$ (Aldrich) dissolved in 25 cm^3 of double-distilled water at room temperature. Excess H_2O_2 was decomposed by contact with Pt foil. The mixed solution was evaporated to dryness in a glass beaker on an electric hot plate. The pinkish paste from the evaporation was heated in air for 1 h at 130 °C to yield a grey-black powder. This powder was ground fine in an agate mortar and pestle, then nitrocarburised as described below.

2.1.2. PPTA precursor

The PPTA precursor was made as follows. Twenty grams of metallic W powder (Alfa) were slowly added to a magnetically stirred solution of 50 cm^3 double-distilled water and 50 cm^3 of analytical grade 30% H_2O_2 at room temperature. With all the powder suspended in solution, another 50 cm^3 of 30% H_2O_2 was added and the stirring continued until all the W had dissolved, leaving a clear solution [18]. Excess H_2O_2 was removed by contacting this solution with a piece of Pt foil overnight and pulling a low vacuum on it to promote gas evolution. Seventy-five cubic centimetres of this clear solution were evaporated to dryness on a hot plate at a temperature of ca. 75 °C. The evaporation yielded 12.71 g of yellow-orange glassy-looking solid PPTA [19] of nominal composition $WO_3{\cdot}0.5H_2O_2{\cdot}2H_2O$. Calcining 7.301 g of this yellow-orange solid in air for 2 h at 300 °C yielded 6.202 g of a fine brownish-yellow solid which showed a Brunauer, Emmett and Teller (BET) surface area of 25.59 m^2/g. X-ray diffraction (XRD) analysis indicated that the calcined product consisted of a mixture of approximately equal proportions of $WO_3{\cdot}0.33H_2O$ [20] and WO_3 [21].

2.1.3. Nitrocarburisation

The WO_3, 1Co2W and PPTA were converted to WC using nitrocarburising. The precursors were heated to 600 °C in a 38 mm diameter electric resistance tube furnace under 100 cm^3/min flow of argon with full furnace power. Typical time to reach 600 °C from room temperature was 20–25 min. At 600 °C, a temperature-programmed reaction (TPR) was begun by switching the furnace atmosphere from argon to 100 cm^3/min NH_3, while ramping the temperature upward at the rate of 2 °C/min until 700 °C was reached. The temperature was held at 700 °C for 30 min with flowing NH_3 in the furnace. Then the NH_3 was valved off and the furnace atmosphere switched to a gas mixture of 20 mol% CH_4/80 mol% H_2 at a flow rate of 83 cm^3/min. The temperature was increased to 827 °C at the rate of 2 °C/min. The furnace was held at 827 °C for 5 min. Then the power was turned off and the mixed gas replaced with a flow of 100 cm^3/min of argon. When the furnace tube reached room temperature, a flow of 100 cm^3/min of argon plus 1% oxygen was introduced into the furnace for 2 h to passivate the sample against pyrophoric combustion before the sample was removed for analysis and examination [22].

2.1.4. Isothermal carburisation

The $NiWO_4$ was carburised by an isothermal treatment for 4 h at 900 °C under a mixed gas of 80 mol% CH_4/20 mol% H_2 flowing at 100 cm^3/min. Afterwards the Ni-doped WC thus synthesised was subjected to reductive hydrogen cleaning as described below, followed by acid treatment in aerated 1.5 M H_2SO_4 for 4 h at 70 °C to leach out free metallic nickel.

2.1.5. Reductive H_2 cleaning

Samples II, IV and V were subjected to a reductive cleaning procedure to rid the surfaces of excess carbon deposited during the thermal synthesis treatment [23]. The samples were loaded into a horizontal tube furnace of 38 mm internal diameter. The furnace was purged with argon at 115 kPa (2 psig) and 100 cm^3/min for 3 h. The gas in the furnace tube was switched to high purity H_2 at 115 kPa (2 psig) and 100 cm^3/min. Under flowing H_2, the temperature was increased to 690 °C at the rate of 35 °C/min and maintained at 690 °C for 1.5 h. Then the power to the furnace was turned off and the gas in the furnace tube switched back to argon. When the furnace reached room temperature, the gas was changed to 1% O_2 in Ar for 2 h to prevent pyrophoric combustion as described above. Sample I (commercial WC) was tested as received and sample III (WC made from the 1Co2W alloy) was tested in the nitrocarburised condition.

After synthesis the powder samples were analysed by XRD using Cu Kα radiation to identify the phases present and measured for specific surface area using nitrogen adsorption with the BET method.

2.2. Electrode fabrication

The powder samples were made into test electrodes [24] as follows. Approximately 0.3 g of the catalyst was weighed, then placed in a 50 cm^3 glass beaker. One cubic centimetre of double-distilled water and 10 cm^3 of analytical reagent grade tetrahydrofuran (THF) were added to the beaker in that order. Polytetrafluoroethene (PTFE) binder was added to this solution as ICI GP-1 solution (54% PTFE by weight, 0.5% surfactants, balance H_2O) in an amount sufficient to give a dry weight of PTFE equal to 16–32% of the catalyst weight. The mixture was stirred ultrasonically for 45 min, with mechanical agitation at 15 min intervals.

Table 1
Electrocatalyst synthesis and electrode fabrication

Electrode no.	Precursor	Synthesis method	Reductive cleaning	BET surface area (m^2/g)	Catalyst loading (g/cm^2)	Binder content (wt.%)
I	JM WC	–[a]	No	0.4	0.061	26.7
II	WO_3	Nitrocarburising	Yes	17.7	0.041	20.3
III	1Co2W	Nitrocarburising	No	4.9	0.058	16.9
IV	PPTA	Nitrocarburising	Yes	17.9	0.021	31.0
V	$NiWO_4$	Isothermal carburising	Yes	1.25	0.049	24.6

[a] Tested as received.

This suspension was applied dropwise to a 25 mm diameter disk of Panex PWB-3 carbon cloth lying on expanded Nb sheet over an electric hot plate. When all the catalyst and binder had been deposited onto the carbon cloth, the disk was pressed and sintered at 20 bar and 360 °C for 30 min between sheets of aluminium foil. Layers of Vulcan PF carbon particles were placed above and below the aluminium foil on both sides of the electrode to cushion the electrode from the stainless steel rams and prevent any sharp catalyst particles from cutting the carbon cloth.

2.3. Electrochemical test procedure

The electrolyte for all tests was 1.5 M H_2SO_4 at 70 °C made from analytical reagent grade acid and double-distilled water. Before testing each electrode was immersed in a beaker of 1.5 M H_2SO_4 at room temperature and evacuated for 30 min to fill the pores of the electrode with acid and remove trapped air.

The electrodes were tested for corrosion currents and electrocatalytic activity potentiostatically. The electrochemical cell was of modular PTFE and glass construction as described previously [25]. The test electrodes had 3.14 cm^2 exposed surface area and a current collector of Au sheet was used. The reference electrode was a mercury–mercurous sulphate (MMS) electrode mounted in a side-arm and connected via an electrolyte-filled tube to the Luggin capillary. Its reference potential, against which the results below are presented, was calibrated as 0.405 V relative to a saturated calomel reference electrode (SCE). All experiments were carried out at a constant temperature of 70 °C. Gas flow into the fuel chamber was held constant at 122 kPa (3 psig) and 20 cm^3/min flow rate.

Potentiostatic tests were carried out as follows. The assembled cell was filled with 1.5 M H_2SO_4 and de-aerated with high purity Ar using a gas-lift pump for 2 h before each test and through the course of each test. Trials with a model 4500 Mettler–Toledo O_2 analyser indicated that this de-aeration procedure reduced the residual O_2 content in the electrolyte to less than 27 ppb by weight.

A series of potentiostatic steps at incremental intervals of 0.1 V covering the electrode potential range from −0.65 to −0.15 V versus MMS was imposed. These were conducted at 70 °C with argon flowing into the fuel chamber to measure the corrosion current as a function of time and potential, using a data acquisition rate of 1 Hz. The potentiostatic transient at each potential was usually conducted for 250 s, although some of the experiments were conducted for considerably longer (see below).

After corrosion testing, another potentiostatic transient was initiated at −0.35 V versus MMS under argon flow. This potential was chosen to give reasonable reaction rates and allow comparison with other base electrocatalysts currently under study. After the passage of enough time to establish the trend of the corrosion current, the argon gas fed to the fuel chamber was replaced by high purity H_2. After some time the high purity H_2 was switched off and a mixed gas of 99 mol% H_2/1 mol% CO (Air Products, Gold Standard grade) was introduced into the fuel chamber. The effect of the CO-bearing gas was measured for times varying from 200 to 1000 s. Then the mixed gas in the fuel chamber was replaced with high purity H_2 to observe the reversibility of the effect of CO. Throughout this procedure the current was recorded continuously.

After the first potentiostatic transient was completed, a series of 250 s potentiostatic current transients were carried out, starting at −0.65 V versus MMS and continuing without interruption at 0.1 V increments, on each electrode, with high purity H_2 in the fuel chamber. Then the series of potentiostatic transients was repeated under the same conditions of temperature, pressure and flow rate using H_2/1% CO gas mixture in the fuel chamber. These tests were conducted on electrodes I–V (Table 1).

The anodic oxidation of CO alone, from a source containing 10% CO/90% N_2, was measured on electrode V.

3. Results and discussion

All current densities are presented relative to the projected surface area, not the true surface area. Fig. 1 presents a typical graph of current density as a function of time, from a potentiostatic transient taken on electrode II. With time the corrosion current falls to very low levels. For example, after 1750 s the measured corrosion current on argon in Fig. 1 was 7 μA/cm^2 of projected electrode area. Since, the electrode had 0.041 g of catalyst/cm^2 of projected electrode area and a measured surface area of 17.7 m^2/g the observed corrosion current of 7 μA/cm^2 of projected electrode area indicates a very low passive corrosion current of 0.96 nA/cm^2 of

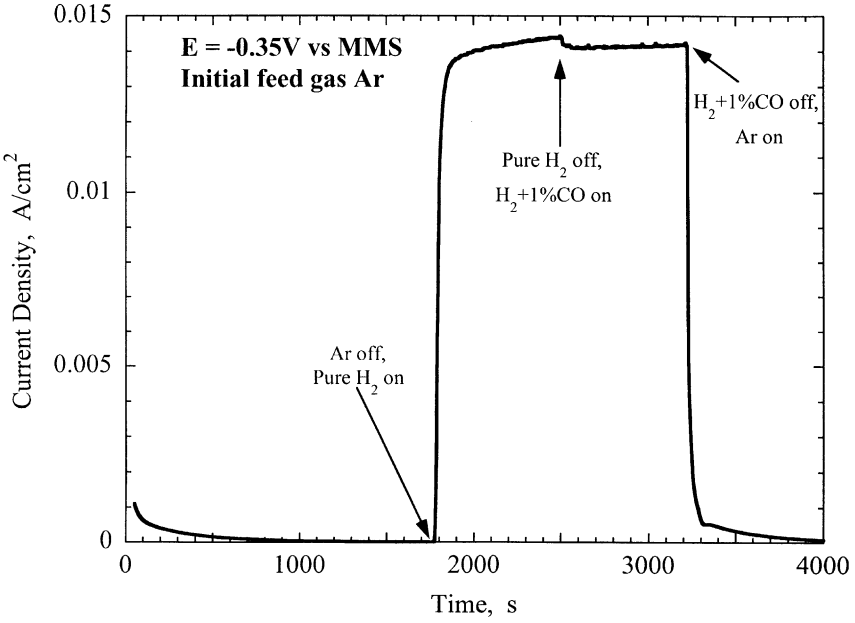

Fig. 1. Current as a function of time at −0.35 V vs. MMS on electrode II (WC made from nitrocarburised WO_3). The first 1750 s were under flow of Ar and show the passivating corrosion current. At 1750 s, pure H_2 was substituted for Ar. At 2500 s, pure H_2 was replaced by 1% CO/99% H_2 gas mixture. At 3200 s, the fuel supply was removed and replaced by Ar.

exposed catalyst surface area. This passive corrosion current is still declining at the end of the observation period. The hydrogen oxidation current is a substantial 14.4 mA/cm^2 of projected electrode area. The hydrogen oxidation current rises as a function of time and continues to do so through the recording period, behaviour observed on all the materials examined except for electrode I (commercial WC). Fig. 1 also shows the typical effect from the presence of CO; a small reduction (∼2.1%) in the magnitude of the H_2 oxidation current. The rate of rise of the H_2 oxidation current was also decreased.

Figs. 2 and 3, from data on tests with electrode III, illustrate the reversibility of the CO effect. The rising oxidation current on pure H_2 is interrupted and reduced

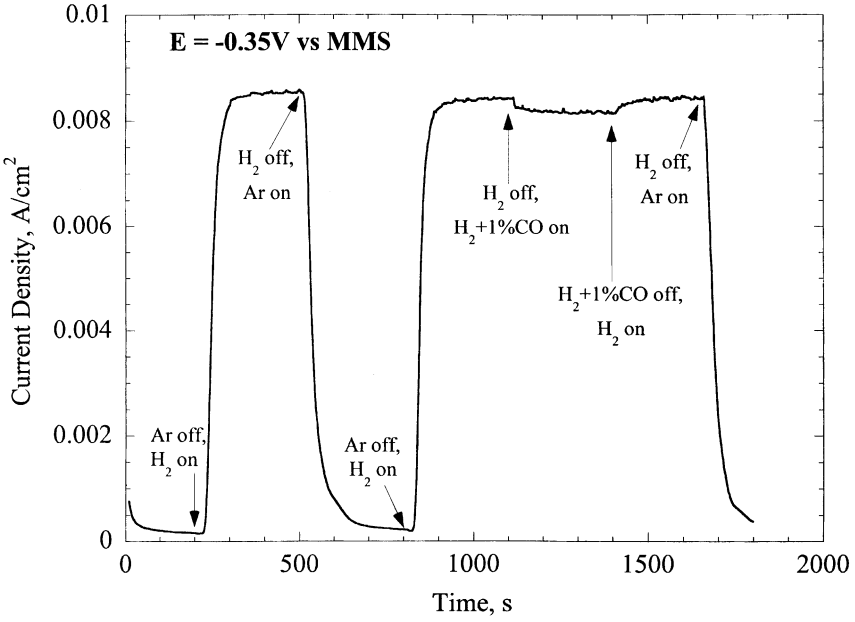

Fig. 2. Current as a function of time at −0.35 V vs. MMS on electrode III (WC made from nitrocarburised 1Co2W). At 200 s, the initial flow of Ar was replaced by pure H_2. At 500 s, H_2 was replaced by Ar. At 800 s, H_2 was re-introduced into the fuel chamber. At 1100 s, pure H_2 was replaced by 1% CO/99% H_2 mixture. The 1% CO/99% H_2 mixture was removed after 1400 s and replaced with pure H_2. At 1650 s, H_2 was removed and Ar was re-introduced into the fuel chamber.

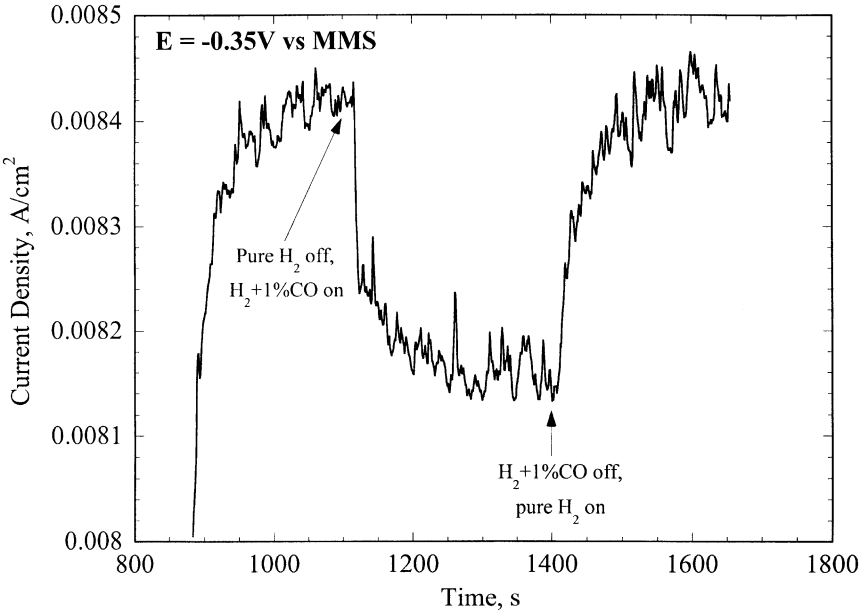

Fig. 3. Detail from Fig. 2, current vs. time from the potentiostatic transient on electrode III, showing the reduction in magnitude and rate of rise of the H_2 oxidation current due to the addition of 1% CO to the feed gas.

by the introduction of 1% CO in the gas mixture. With CO in the gas, the current falls but by only about 3% and levels off instead of continuing to increase. When the CO is removed from the gas mixture, the H_2 oxidation current rises to its earlier levels and continues to increase with time, returning the electrode to its prior state.

Fig. 4 summarises the effect of CO on the observed H_2 oxidation currents. The graph shows the percent change in anodic H_2 oxidation current upon the admission of the 1% CO gas mixture as a function of electrode potential. For all these materials, at most electrode potentials, the presence of CO in the H_2 causes a reduction of between 2 and 6% in the observed oxidation current. The open-circuit potential (OCP) of each material was measured as between −0.668 and −0.680 V versus MMS in all cases where H_2 was present. We regard these OCP values as dominated by the H_2/H^+ equilibrium.

Fig. 5 presents data describing the anodic oxidation of CO alone on electrode V (WC made from $NiWO_4$). The feed gas was 10% CO in N_2. These data are plotted together with

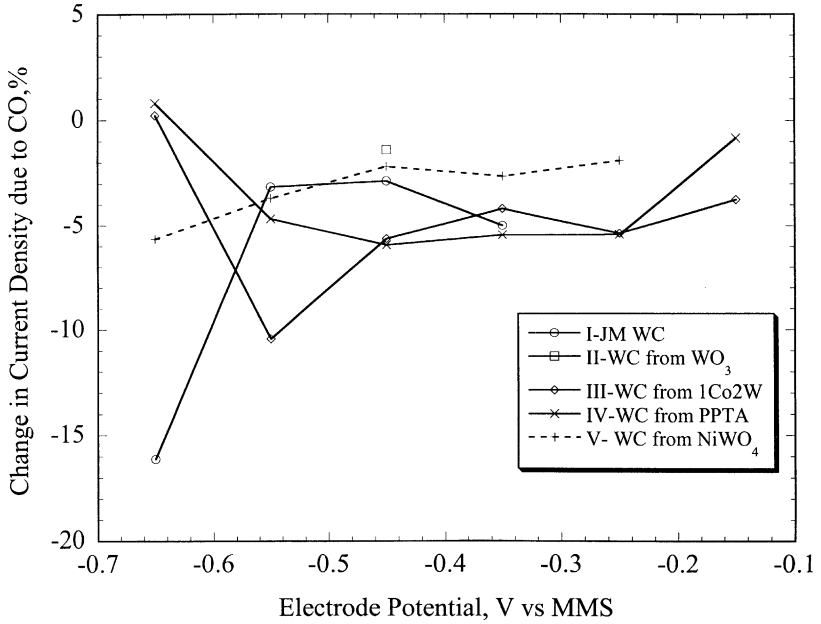

Fig. 4. Graph showing the effect of 1% CO on WC, the percentage change in observed H_2 oxidation current density after 250 s, as a function of material and electrode potential.

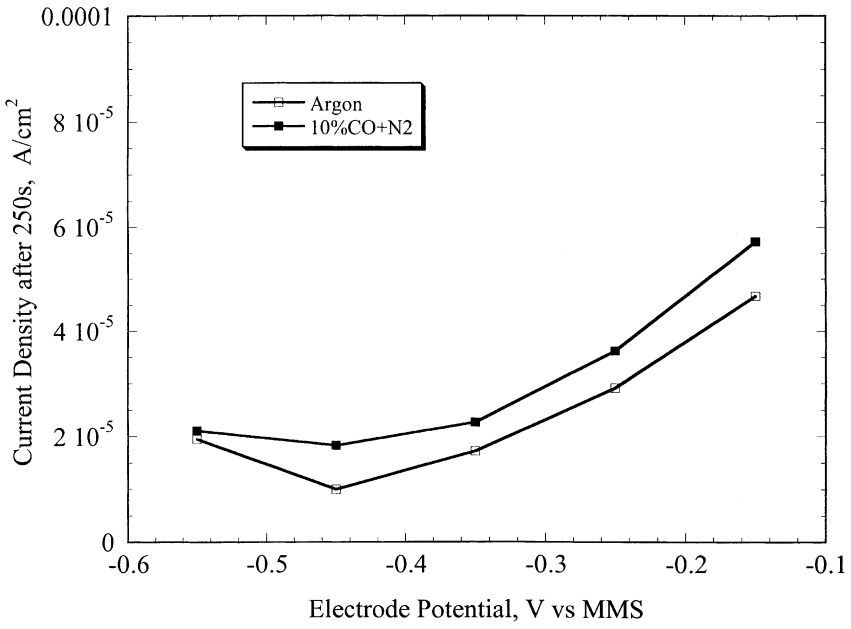

Fig. 5. Polarisation of electrode V (WC from carburised $NiWO_4$), comparing the current density observed when using 10% CO in N_2 feed gas with baseline corrosion data obtained under argon.

those obtained under argon for comparison. The CO mixture produces only a very small increase in observed anodic current above the argon baseline. The average increase is 6.6 μA/cm^2 of projected electrode area, across the potential range −0.55 to −0.15 V versus MMS. Assuming that the N_2 in this gas mixture is inert, these data show that CO is oxidised only at very low rates on WC. The current due to anodic oxidation of CO is less than 0.1% of the H_2 oxidation current on the same electrode.

With argon as the feed gas, electrodes III and V (WC samples made from $NiWO_4$ and 1Co2W) showed initially high corrosion currents, on the order of several mA/cm^2, which declined with time to <0.2 μA/cm^2. Energy dispersive X-ray analysis (EDX) after testing indicated that almost all the Ni and Co were dissolved out of these materials, leaving <0.5 at.% of the alloying additions after exposure to the acid. At these levels the Ni and Co additions appeared to have little effect on the hydrogen oxidation reaction, since electrodes III and V gave OCP values equivalent to those of the WC samples without alloy additions and their polarisation curves showed the same shapes as the WC samples free of Ni and Co. In essence all the materials behaved as if they were simply WC of different surface areas. When calculated as a percentage of the H_2 oxidation current, the CO poisoning effect was remarkably similar for all these materials and independent of electrode potential.

It will be noted that, in Fig. 4, at low potentials, electrodes I and III show one datum each with slightly more CO poisoning than the common trend. Both these materials were tested in the carburised condition, with no reductive cleaning, so it may be that surface contaminants of the catalyst particles, most probably deposited carbon, produced slightly more CO adsorption and thus, more poisoning than observed in the rest of this study. The effect is not seen at all potentials and may well be the result of surface contamination which is removed by longer term polarisation.

The reversibility of the CO effect on WC and the low anodic oxidation rate of CO suggest that CO must be very weakly adsorbed on WC surfaces. The CO therefore masks very few of the catalytic sites during oxidation of H_2 and its desorption on removal of the CO supply is facile.

4. Conclusions

1. WC shows a small and reversible reduction in the magnitude and rate of rise of the hydrogen oxidation current when 1% CO is added to a hydrogen fuel gas.
2. On WC electrocatalysts, the reduction in H_2 oxidation rate due to the presence of CO is ∼2–6%.
3. The rate of anodic oxidation of CO on WC is very low (<0.1% of the H_2 oxidation currents).
4. The effect of CO on WC appears to be independent of electrode potential and independent of synthesis route.
5. The effect of CO on WC appears to be the result of very weak surface adsorption which temporarily blocks the most active catalytic sites for H_2 oxidation.

References

[1] A.B. Hart, G.J. Womack, Fuel Cells: Theory and Application, Chapman & Hall, London, 1967, p. 155.
[2] J.W. Pearson, in: K.R. Williams (Ed.), An Introduction to Fuel Cells, Elsevier, Amsterdam, 1966, p. 292.

[3] P. Stonehart, P.N. Ross, Catal. Rev. Sci. Eng. 12 (1975) 1.
[4] M.T. Paffett, E. Ticianelli, S. Gottesfeld, in: Proceedings of the 1988 Fuel Cell Seminar, National Fuel Cell Coordinating Group, Long Beach, CA, 23–26 October 1988, p. 126 (Abstract).
[5] T.J. Schmidt, H.A. Gasteiger, R.J. Behm, Electrochem. Commun. 1 (1999) 1–4.
[6] P.G. Gray, M.I. Petch, Platinum Met. Rev. 44 (3) (2000) 108–111.
[7] R. Noyes, Fuel Cells for Public Utility and Industrial Power, Noyes Data Corp., Park Ridge, NJ, 1977, p. 142.
[8] P.N. Ross, P. Stonehart, J. Catal. 48 (1977) 42–59.
[9] A.J. McAlister, L.H. Bennett, M.I. Cohen, in: Proceedings of the National Fuel Cell Seminar, Hyatt Regency Hotel, San Francisco, CA, 11–13 July 1978, p. 169 (Abstract).
[10] H. Böhm, F. Pohl, J. Inst. Etudes Piles a Combustibles, Brussels, June 1969, pp. 183–186.
[11] L. Baudendistel, H. Böhm, J. Heffler, G. Louis, F.A. Pohl, in: Proceedings of the 7th International Energy Conversion Engineering Conference, American Chemical Society, Washington, DC, September 1972, Paper no. 729004.
[12] G.V. Biokova, G.V. Zhutaeva, M.R. Tarasevich, Soviet Electrochem. 23 (7) (1987) 822–828.
[13] G. Bronoel, E. Museux, G. Leclercq, L. Leclercq, N. Tassin, Electrochim. Acta 36 (10) (1991) 1543–1547.
[14] G.A. Tsirlina, O.A. Petrii, V.B. Kozhevnikov, Soviet Electrochem. 20 (3) (1984) 397–400.
[15] G.A. Tsirlina, O.A. Petrii, Electrochim. Acta 32 (1987) 649–657.
[16] R. Fleischmann, H. Böhm, Electrochim. Acta 22 (1977) 1123–1128.
[17] L. Volpe, M. Boudart, J. Solid State Chem. 59 (1985) 348.
[18] H. Nakajima, T. Kudo, N. Mizuno, Chem. Lett. (1997) 693–694.
[19] W. Han, M. Hibino, T. Kudo, Bull. Chem. Soc. Jpn. 71 (1998) 933–937.
[20] W.F. McClune (Ed.), Inorganic Phases: Alphabetical Indices to the Powder Diffraction Files, International Centre for Diffraction Data, Newtown, PA, 1999, PDF no. 35-0270.
[21] W.F. McClune, op. cit. [16], PDF no. 43-1035.
[22] J.H. Kim, K.L. Kim, Appl. Catal. A Gen. 181 (1999) 103–111.
[23] G. Leclercq, M. Kamal, J.F. Lamonier, L. Feigenbaum, L. Malfoy, P. Leclercq, Appl. Catal. A Gen. 121 (1995) 169–190.
[24] G.T. Burstein, C.J. Barnett, A.R.J. Kucernak, K.R. Williams, J. Electrochem. Soc. 143 (1996) L139.
[25] C.J. Barnett, G.T. Burstein, A.R.J. Kucernak, K.R. Williams, Electrochim. Acta 42 (1997) 2381.